



Calhoun: The NPS Institutional Archive
DSpace Repository

Theses and Dissertations

1. Thesis and Dissertation Collection, all items

1972

An optical object detection system for sensing obstructions to low speed vehicles

Burman, George Alfred

Monterey, California. Naval Postgraduate School

<http://hdl.handle.net/10945/16285>

Downloaded from NPS Archive: Calhoun



<http://www.nps.edu/library>

Calhoun is the Naval Postgraduate School's public access digital repository for research materials and institutional publications created by the NPS community. Calhoun is named for Professor of Mathematics Guy K. Calhoun, NPS's first appointed -- and published -- scholarly author.

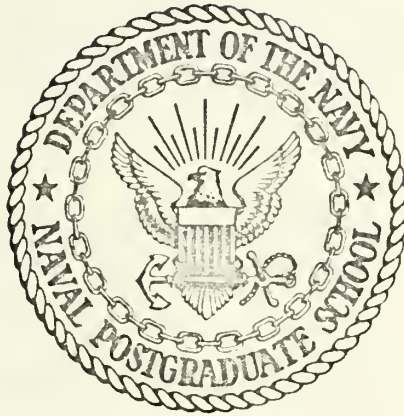
Dudley Knox Library / Naval Postgraduate School
411 Dyer Road / 1 University Circle
Monterey, California USA 93943

AN OPTICAL OBJECT DETECTION SYSTEM
FOR SENSING OBSTRUCTIONS
TO LOW SPEED VEHICLES

George Alfred Burman

NAVAL POSTGRADUATE SCHOOL

Monterey, California



THESIS

AN OPTICAL OBJECT DETECTION SYSTEM
FOR SENSING OBSTRUCTIONS
TO LOW SPEED VEHICLES

by

George Alfred Burman

Thesis Advisor

G. L. Sackman

June 1972

T148517

Approved for public release; distribution unlimited.

An Optical Object Detection System
for
Sensing Obstructions to Low Speed Vehicles

by

George Alfred Burman
Lieutenant, United States Navy
B.S., California State Polytechnic College, 1963

Submitted in partial fulfillment of the
requirements for the degree of

MASTER OF SCIENCE IN ELECTRICAL ENGINEERING

from the

NAVAL POSTGRADUATE SCHOOL
June 1972

ABSTRACT

An object detection system to sense obstructions in the path of low speed vehicles is described. The system uses a pulsed GaAs diode laser as an illuminator, and a PIN photodiode as a detector. Reliable detection of objects with an effective area as small as 0.5 ft^2 was achieved. A signal processor using active filters and a phase-locked loop tone decoder was employed for both phase and frequency rejection of undesired signals, and detection of objects under high ambient light conditions.

TABLE OF CONTENTS

| | | |
|-----|--|----|
| I. | INTRODUCTION----- | 7 |
| II. | DETAILED SYSTEM DESCRIPTION ----- | 13 |
| A. | TRANSMITTER ----- | 13 |
| 1. | Laser Pulsing Considerations----- | 13 |
| 2. | SCR Pulsing Circuit ----- | 14 |
| 3. | Trigger Circuit ----- | 18 |
| 4. | Charging Circuit ----- | 18 |
| 5. | Optics----- | 19 |
| 6. | Safety Considerations ----- | 20 |
| B. | RECEIVER ----- | 20 |
| 1. | Optics----- | 20 |
| 2. | Photodiode Considerations----- | 22 |
| 3. | Impedance Converter ----- | 23 |
| 4. | Preamplifier----- | 25 |
| 5. | Power Supply ----- | 26 |
| C. | SIGNAL PROCESSING SECTION----- | 26 |
| 1. | General ----- | 26 |
| 2. | Active Filter----- | 27 |
| 3. | Phase-Shifter, Buffer, and Limiter ----- | 31 |
| 4. | Tone Decoder ----- | 32 |

| | |
|--|----|
| III. TEST RESULTS | 35 |
| A. RANGE TESTS | 35 |
| 1. Reflection Tests | 35 |
| 2. Target Response | 37 |
| 3. Direct Line-of-Sight Tests | 37 |
| B. SPURIOUS RESPONSES | 41 |
| 1. Ambient Light | 41 |
| 2. Dust and Smoke | 41 |
| 3. Electromagnetic Compatability | 42 |
| 4. Adjacent Transmitter Interference | 42 |
| IV. CONCLUSION | 44 |
| A. RANGE RESPONSE | 44 |
| B. TARGETS | 45 |
| C. ENVIRONMENTAL CONDITIONS | 45 |
| APPENDIX A Photographs of Various Voltage and Current Waveforms | 46 |
| APPENDIX B Active Filter Frequency Response | 49 |
| BIBLIOGRAPHY | 50 |
| INITIAL DISTRIBUTION LIST | 51 |
| FORM DD 1473 | 52 |

LIST OF DRAWINGS

| | |
|--|----|
| 1. Desired Detection Zone ----- | 8 |
| 2. Detection Zones Formed by Transmitter-Receiver Pairs----- | 10 |
| 3. Transmitter-Receiver Block Diagram----- | 11 |
| 4. Normalized Threshold Current vrs. Junction Temperature --- | 15 |
| 5. Transmitter Schematic ----- | 16 |
| 6. Transmitter Beam Optics ----- | 19 |
| 7. Receiver Optics ----- | 21 |
| 8. Photodiode Impedance Converter and Preamplifier Schematic - | 24 |
| 9. Photodiode and Impedance Converter Equivalent Circuit----- | 23 |
| 10. Signal Processor Block Diagram ----- | 28 |
| 11. Spectral Content of Fluorescent Lights ----- | 30 |
| 12. Active Filter Schematic ----- | 29 |
| 13. Phase-Shifter, Buffer, and Limiter Schematic ----- | 31 |
| 14. Tone Decoder Schematic----- | 32 |
| 15. Range Response of a 1 ft ² Target ----- | 36 |
| 16. Direct Line-of-Sight Range Response ----- | 40 |
| 17. Radiated Interference Spectrum ----- | 43 |

ACKNOWLEDGEMENTS

The author wishes to thank Professor George L. Sackman, for his assistance as Thesis Advisor, and for the original formulation of the system concept; the Hewlett Packard Corporation and the Signetics Corporation for providing components and technical assistance; and his wife, Martha, for typing and assistance in taking data.

I. INTRODUCTION

An object detection system was required for low speed cargo vehicles, similar to fork-lifts, to prevent personnel and equipment injury. The vehicles operate in a long warehouse corridor, and are programmed for automated loading and unloading of bins on both sides of the corridor.

The system described will detect objects, such as personnel, boxes, crates, or other items that accidentally come into the path of the vehicle.

One requirement for the system was that the detection zone cover a large area, have sharply defined edges, and have limited range. As a result, a simple optical beam breaking alarm, or ultrasonic intrusion type alarm could not be used.

The detection zone required is shown in Figure 1. Since there is no likelihood that an obstruction would be suspended from the roof of the corridor, with no support from floors or walls, the detection zone can attain the "U" shape shown.

In order to limit the range of detection to approximately 12 feet, so that two vehicles might operate in the same corridor without mutual interference, the one horizontal and two vertical portions of the detection zone were composed of pairs of illuminators and detectors, separated by the width or height of the vehicle so that only an

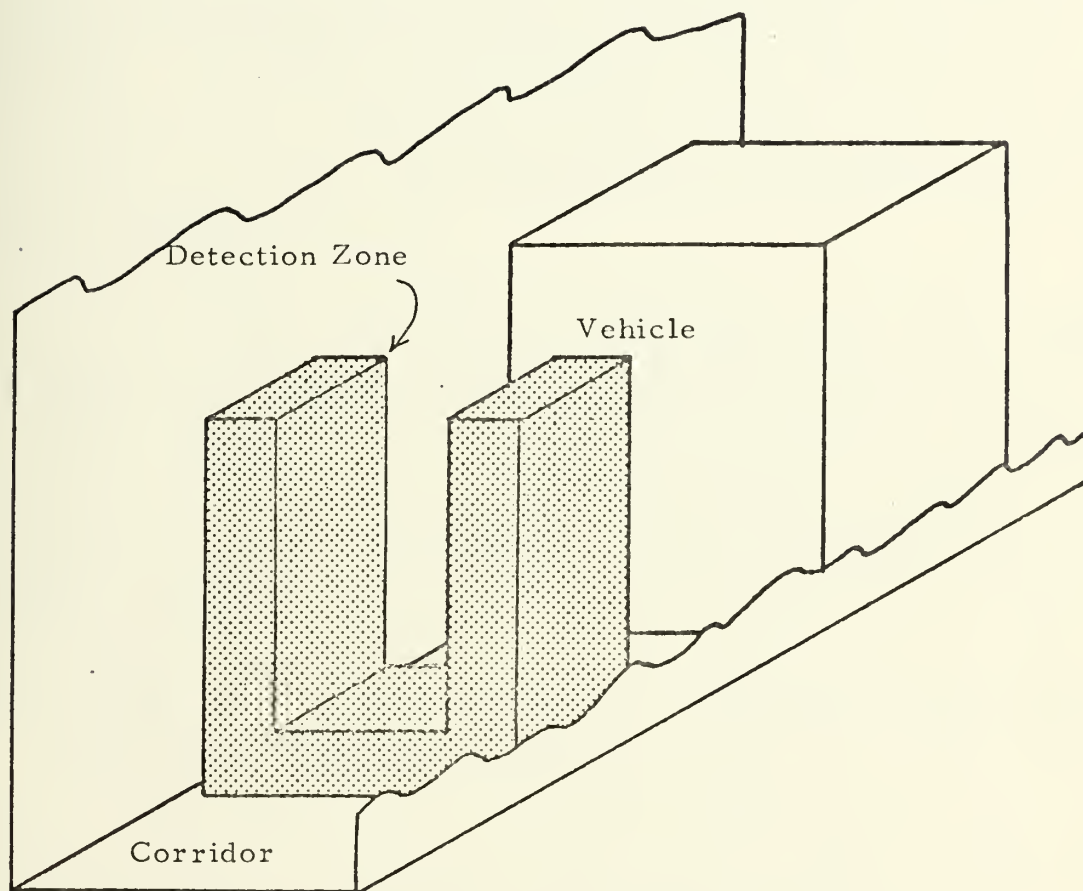


Figure 1. Desired Detection Zone

object lying in both the illumination beam, and within the receiver acceptance cone, would be detected. The pattern of overlapping areas to form either the horizontal or vertical portions of the detection zone is shown in Figure 2.

In Figure 2, T_1 , R_1 , T_2 , R_2 , etc, represent transmitter-receiver pairs operating with different pulse repetition frequencies (PRF), so that R_2 will respond only to a target illuminated by T_2 , and not by T_1 or T_3 . An additional three transmitter-receiver pairs fill in the zone denoted by T'R'. A block diagram of a transmitter-receiver pair is shown in Figure 3.

If the detection zone depth could be extended to 21 feet, as shown in Figure 2, the signal processing and phase-locked-loop detector could be common to three transmitter-receiver pairs, thereby reducing cost and size of the system. The T'R' pairs still must operate on different frequencies, as must the transmitter-receiver pairs composing the other two segments of the overall detection zone.

A near infrared GaAs laser diode was chosen for the illumination source, because of its low cost, small size, and relatively high power output (as compared to LED's). Power supply requirements for the transmitter are modest, requiring only 1.5 watts average power (300 volts at 5 ma). In addition, a -15 volt source is required for the transmitter, which is obtained from the receiver power supply.

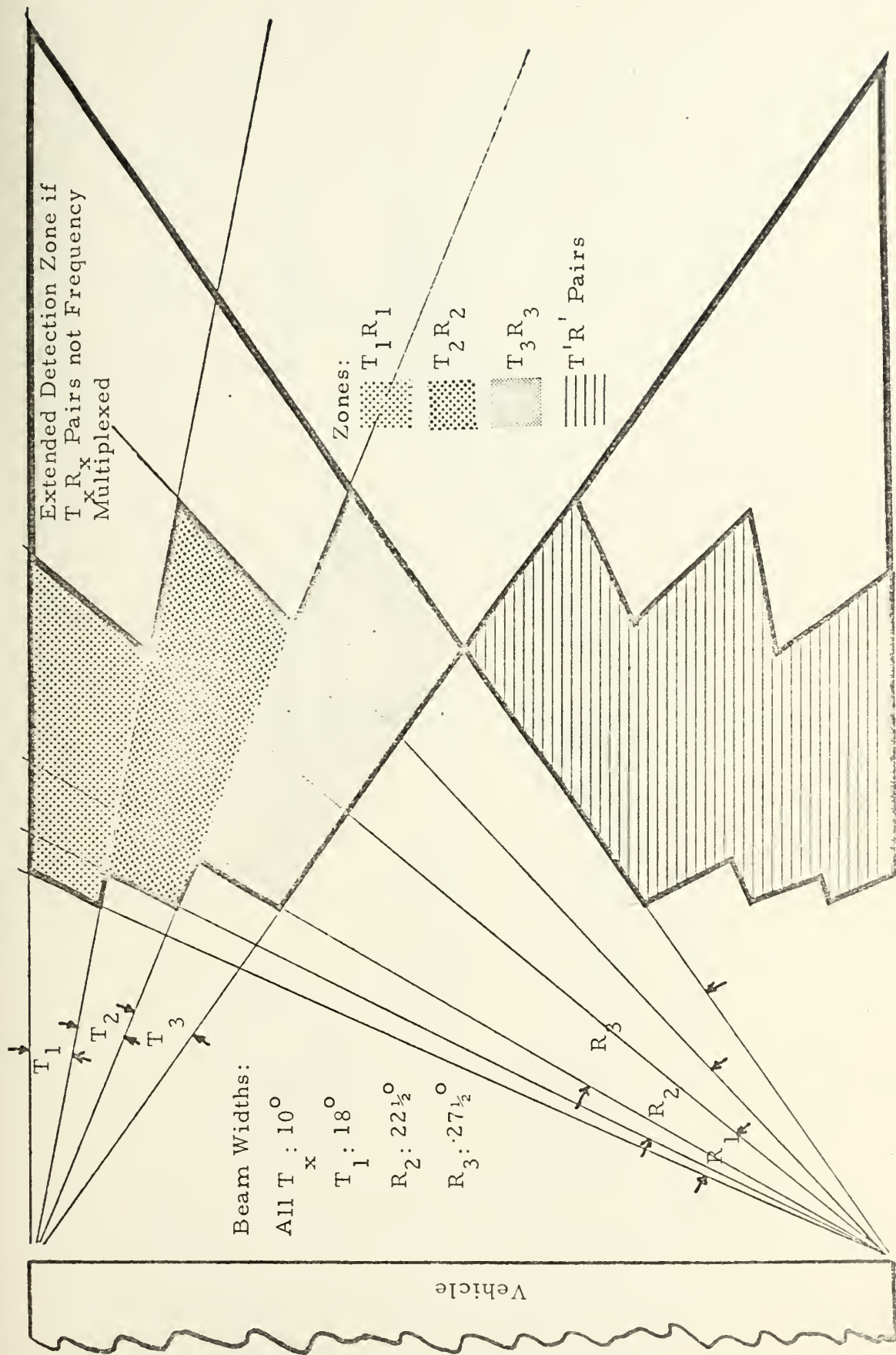


Figure 2. Detection Zones Formed by Transmitter-Receiver Pairs

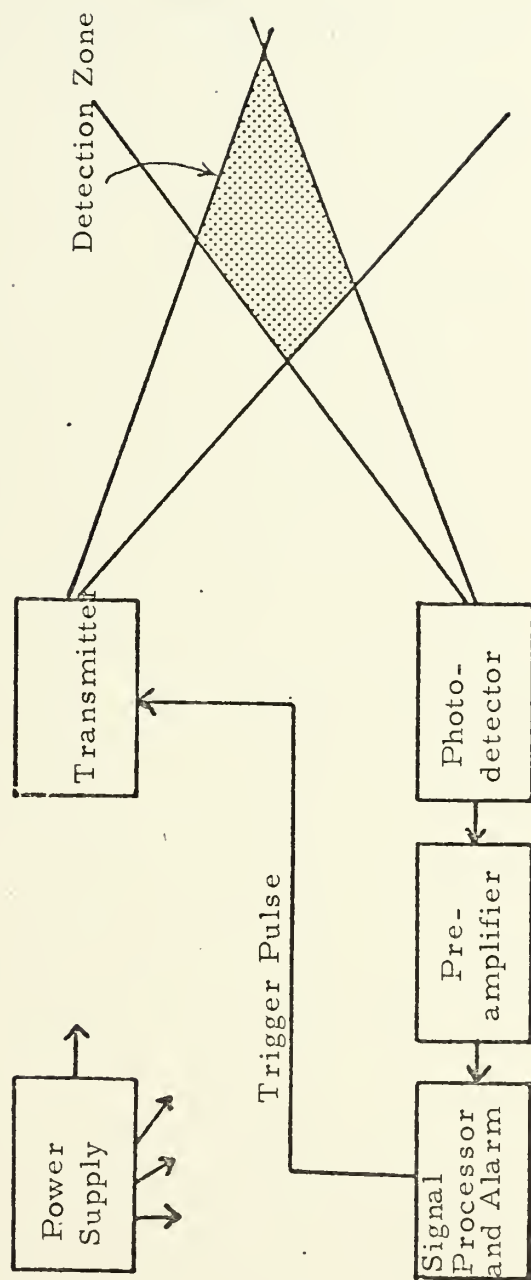


Figure 3. Transmitter-Receiver Block Diagram

The receiver employs a PIN photodiode for a detector, and, with the exception of the first stages of the receiver, integrated circuits were employed. The entire receiver operates from a dual ± 15 volt supply, which draws 25 mA per side.

II. DETAILED SYSTEM DESCRIPTION

A. TRANSMITTER

1. Laser Pulsing Considerations

The laser employed in this system is a Laser Diode Laboratories Model LD-22. This diode is a gallium arsenide injection device which emits coherent infrared radiation when suitably pulsed. The diode is built as a hetero-structure, which differs from older diffused junction devices in that three distinct layers: n-type gallium arsenide, p-type gallium arsenide, and p-type gallium aluminum arsenide compose the diode structure. The hetero-junction is formed at the interface of the p-type gallium arsenide, and the p-type gallium aluminum arsenide, which serves to confine the injected electrons and reduce reabsorption. These devices are more efficient than diffused junction devices since the current at which lasing action occurs (threshold current) is lowered. Radiation is along the axis of the hetero-junction and is proportional to the forward current of the diode.

Peak Power: 6 Watts

Threshold current: 8 Amperes

Peak forward current: 25 Amperes

Table I.

The laser diode can only be operated in a pulsed mode, since current pulses of more than 200 nanosecond duration would overheat the junction and destroy the device. Specifications for the LD-22 limit the PRF to 5MHz, and pulse width to 200 nanoseconds.

A more important consideration is the shape of the current pulse. Threshold current increases with junction temperature, as shown in Figure 4.

If the pulsing current waveform does not have a fast rise time, the current flowing below threshold level will not cause lasing action, but will only heat the junction, thereby raising the threshold level and decreasing efficiency.

2. SCR Pulsing Circuit

In order to generate a current pulse of sufficient magnitude, and which has a fast rise-time, a capacitor discharge circuit employing a fast SCR was used. The circuit used is shown in Figure 5. The SCR switch is an RCA 40768. In pulse circuits of this type, the SCR is operated in an unconventional mode, i. e., the duration of the anode current pulse is much less than 1 microsecond, (nominal turn-on time for most SCR's). In the conventional mode, turn-on impedance is a fraction of an ohm. However, in the laser pulser, the capacitor discharges in less than one microsecond, so that the SCR does not completely turn on, and the anode-to-cathode impedance can attain a level of several ohms during the conduction period. This impedance considerably increases the voltage required to pulse the laser at the

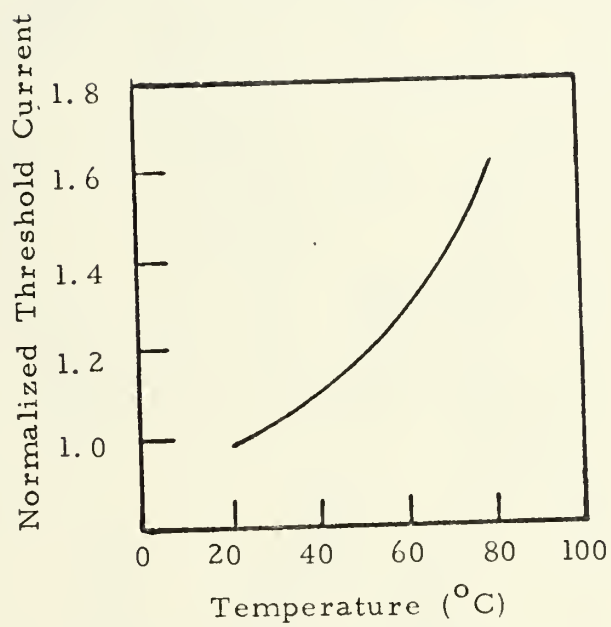


Figure 4. Normalized Threshold Current
vrs. Junction Temperature

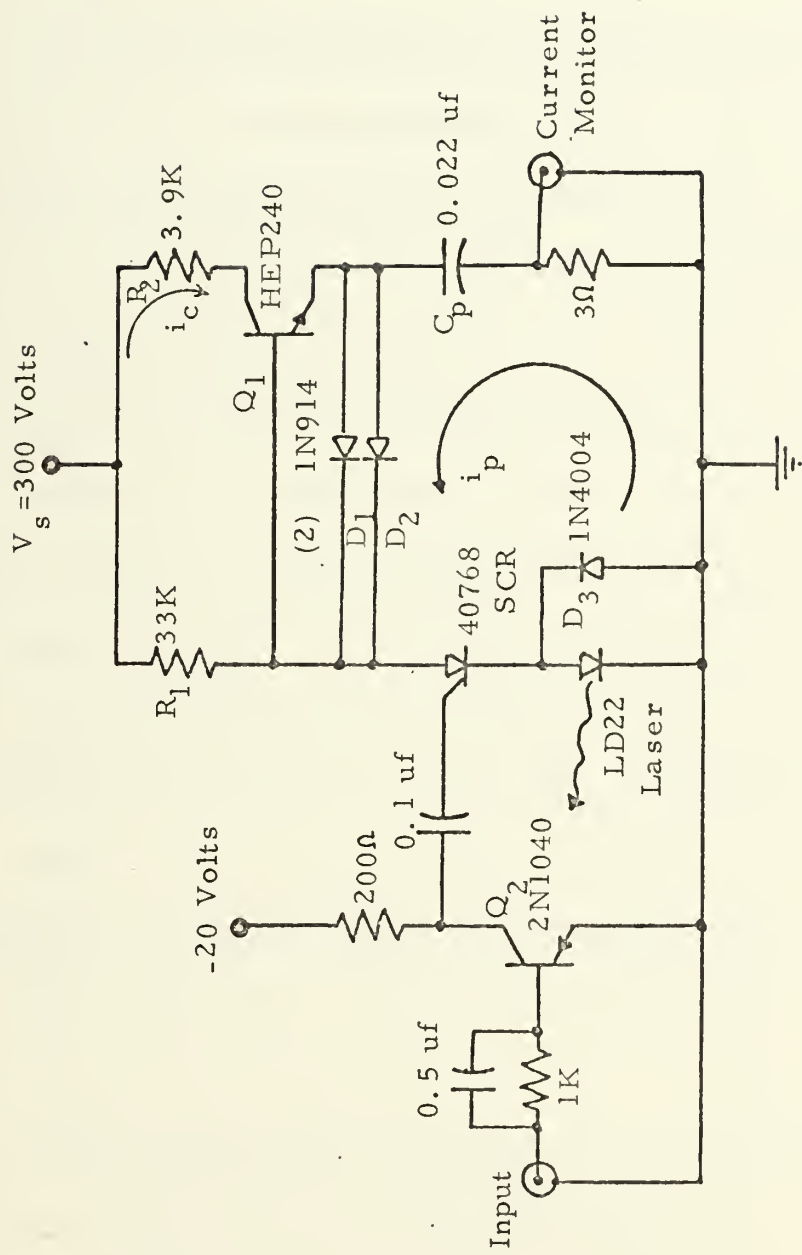


Figure 5. Transmitter Schematic

required current levels. The laser diode exhibits a forward resistance of much less than one ohm. The only other resistive element of the pulsing circuit is the current monitor resistor which was selected at 3 ohms.

Reactance in the pulsing circuit, from lead inductance and wiring capacitance, can cause ringing in the current pulse. The SCR turn off time is much longer than the ringing time, and voltage transients in excess of 3 volts of reverse bias can destroy the laser diode. Excessive wiring capacitance will reduce the slope of the current pulse, thereby reducing laser efficiency because of junction heating.

Selection of an SCR cannot be made on the basis of published data alone. These data give characteristics of the SCR in a gross sense, and do not indicate performance in high speed pulsing applications. Recommended selection is on the basis of a "use test"; the RCA 40768 can be depended on to fulfill the requirements for laser pulser service. Reference 8 claims the RCA GA-201 will work in a laser pulser circuit with the high voltage supply requirement reduced to 100 volts. The GA-201 was not available for use, so the 40768 was used.

Circuit layout in the pulsing circuit is critical. Resistance in the pulsing circuit, which is composed of SCR conduction resistance, laser resistance, current monitor resistance, control diode (1N914) resistance, will all tend to dampen out ringing. If the sum of these

resistances is too low, negative voltage overshoots can destroy the laser; if the resistance is too large, pulsing efficiency is reduced. Diode D_3 also protects the laser from reverse bias damage.

3. Trigger Circuit

The 40768 SCR requires a trigger pulse of 10 ma, with a duration of at least 1 microsecond. The gate to cathode impedance is low, so the trigger source must be obtained from a low impedance source. A simple common-emitter amplifier was constructed so that a readily available pulse generator (GR 1217-C) might be used. In the final design, trigger pulses are obtained from the phase locked-loop tone decoder. A description of the required waveshaping to obtain these pulses is described in section II. C. 4.

4. Charging Circuit

The capacitor (C_p) which delivers the current pulse to the laser must be re-charged between successive pulses. However, before the capacitor is recharged, the SCR must be turned off, otherwise current would flow continuously through the laser after the initial pulse. The holding current for the 40768 is nominally 25 ma. Resistor R_1 of Figure 5 limits the steady-state current from the 300 volt supply to 8.5 ma, which is well below the holding current. Thus, the SCR is forced to open once the current falls below 25 ma.

Diodes D_1 and D_2 , due to their forward voltage drop of approximately 1.2 volts, hold Q_1 in a cutoff state as long as current flows through the SCR. When the SCR opens, Q_1 is then biased into

saturation and the capacitor C_p charges through R_2 . Since the $R_2 C_p$ time constant is 86 microsecond, much less than the pulsing period of 1 millisecond, C_p charges to the full 300 V before the next pulse occurs.

Pulse current control is obtained by varying the high voltage supply, V_s . For full rated output of the LD-22, V_s is set to 300 volts. Reference 7 shows alternate methods of adjusting pulse current.

Waveforms of i_p and v_{c_p} are shown in Appendix A.

5. Optics

The radiated emission of the LD-22 is confined to a cone of 15° at the 3 dB points. Since it was desired to shape the beam into a fan with minimum vertical dispersion, and 10° horizontal dispersion, a cylindrical lens of 25mm focal length was employed to collimate the beam vertically, and the horizontal plane was masked with an aperture to the 10° beam width. Vertical collimation was expected to give a $1/R^3$ response to the system rather than a $1/R^4$ response. A diagram of the lens system is shown in Figure 6.

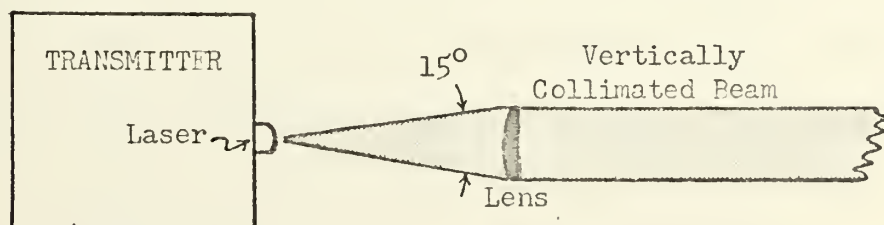


Figure 6. Transmitter Beam Optics

6. Safety Considerations

Reference 1 states that the maximum safe light intensity of a pulsed laser with very short pulse duration, and operating in the near infrared (where the light is focused on the retina of the eye), is 0.07 joules/cm². With a laser output of 5 watts, the maximum power density at the surface of the cylindrical lens is 11.94 watts/cm². Converting this to an energy density, by multiplying by the pulse duration, yields a density of 2.388×10^{-6} joules/cm², which is well below the maximum safe level. The laser should therefore present no safety hazard to personnel.

B. RECEIVER

1. Optics

The laser pulses reflected from an obstruction in the detection zone were focused on the detector cell by means of a condensing lens onto a translucent mylar integrating surface. This is shown in Figure 7.

The PIN photodiode used, an HP4203, has an acceptance angle of 90°. Since the desired field of view of the receiver ranges from 18° to 27½°, considerable receiver aperture gain could be realized by optical focusing as opposed to simple masking of the receiver aperture. The lens employed is a 30 mm diameter, 55 mm focal length (f/1.83) lens.

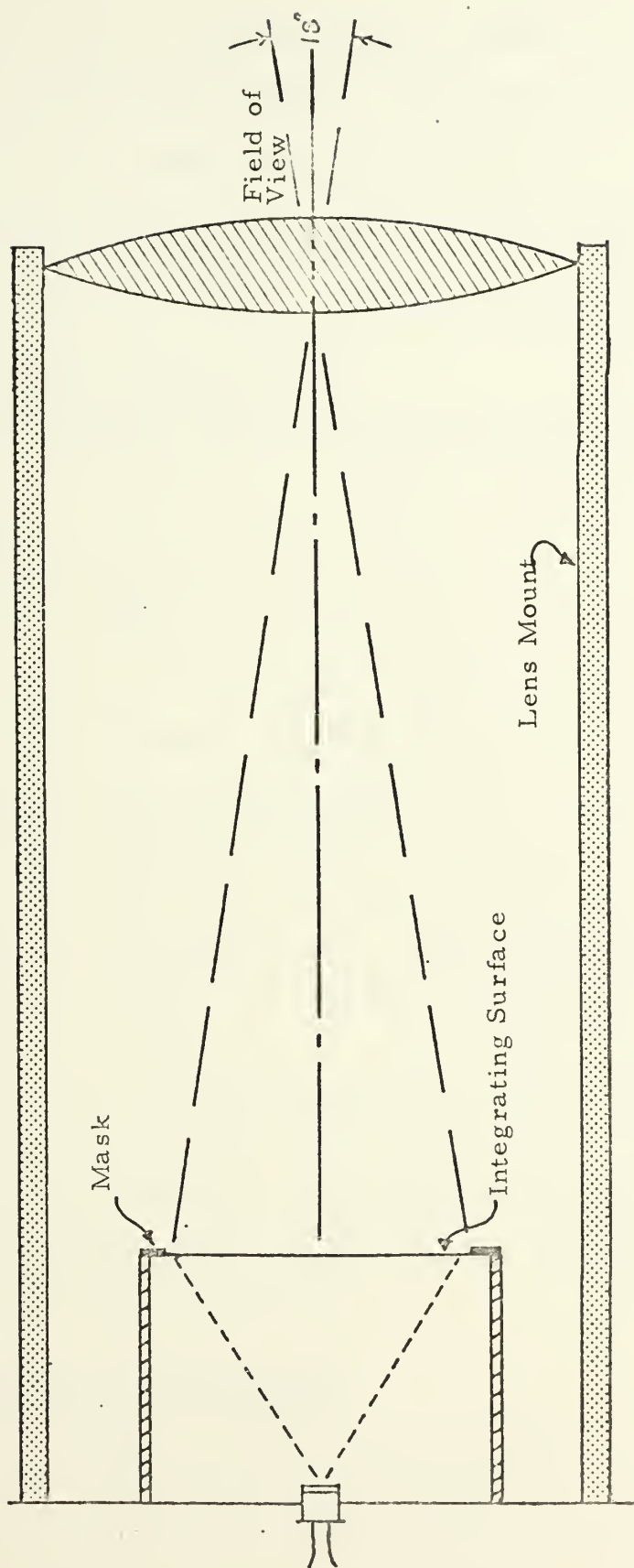


Figure 7. Receiver Optics

The integrating surface was masked to provide the desired field of view. With a 17 mm width of the integrating surface, field of view is 18° , as shown in Figure 7. This is the field required for R_1 . For R_2 and R_3 , wider integrating surfaces are required. Vertical masking height is relatively unimportant, since the transmit beam is collimated in the vertical plane, but should be as large as practical in order to maximize optical gain.

The optical gain of the receiver can be expressed by the relation:

$$G_r = \frac{A_1}{A_d} \rho$$

where

G_r = Receiver optical gain

A_1 = Lens aperture area

A_d = Photodiode aperture surface

For a 30 mm diameter lens, and photodiode area of 0.2 mm^2 ,

$$G_r = \frac{706.86}{0.2} \rho = 3534.3 \Rightarrow 35.5 \text{ dB} + \rho (\text{dB})$$

Since $\rho < 1$, the gain will be less than 35.5 dB. The value of ρ depends on many factors, including reflection and transmission qualities of the lens system, and losses due to masking. An empirical value of ρ is given in section III.A.3.

2. Photodiode Considerations

The PIN photo diode detector (HP 4203) is a silicon planar device sensitive to visible and near-infrared radiation. These devices

exhibit response speeds of less than 1 nanosecond, and have a low dark current (5000 picoamp) which allow detection of low light levels. The quantum detection efficiency is constant over 6 decades of light intensity, which provides a 60 dB dynamic range. All of these features make this type of device especially suitable for application in a system to detect short duration laser pulses in a high ambient light level environment.

3. Impedance Converter

The PIN photodiode can be considered a current source with a source impedance of 22 Megohms. It is therefore essential to operate the photodiode into a very high impedance load. A FET source follower circuit was used, shown in Figure 8.

An equivalent circuit for the photodiode and impedance converter is shown in Figure 9. Where i_p is the photo current, i_n is

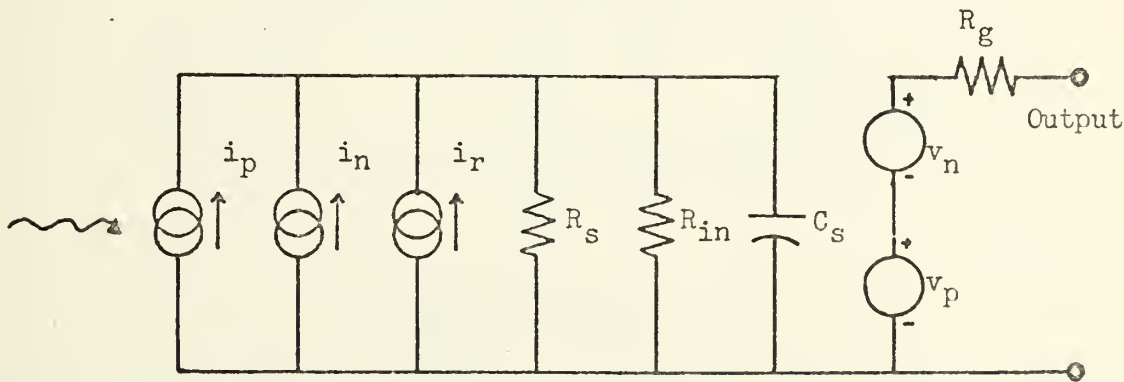


Figure 9

Photodiode and Impedance Converter
Equivalent Circuit

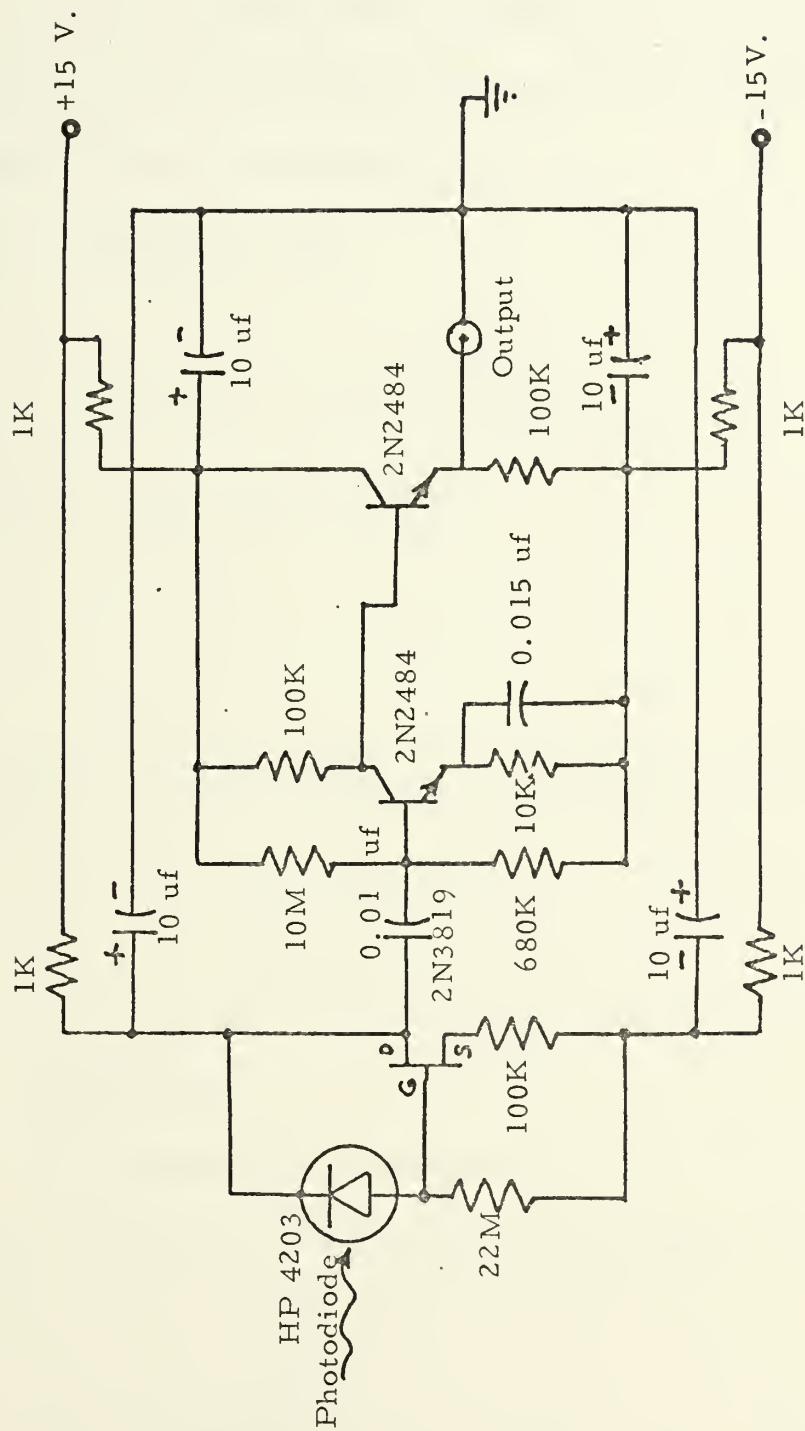


Figure 8. Photodiode Impedance Converter and Preamplifier Schematic

the noise current of the photodiode, i_r is the dark current, R_s is the equivalent source resistance of the photodiode (22 megohm), R_{in} is the input resistance of the impedance converter, C_s is the shunt capacitance of the photodiode and circuit capacitance, v_n is the noise voltage of the FET, and v_p is the voltage response of the impedance converter. The output voltage is the sum of v_n and v_p :

$$v_{out} = v_n + v_p$$

where

$$v_p = (i_p + i_n + i_r) \frac{R_s R_{in}}{R_s + R_{in}}$$

For relative by high signal intensity:

$$i_p \gg i_n$$

and

$$i_p \gg i_r$$

The input impedance of a MOSFET is nearly infinite, so

$$R_s \parallel R_{in} \approx R_s, \text{ and}$$

$$v_p \approx i_p R_s$$

which, in this case, is 22 microvolts per picoamp.

4. Preamplifier

The preamplifier is a simple, two stage section employing low-noise transistors. The first stage is a common-emitter configuration, and is only remarkable in that the input impedance is higher than usual, so that the impedance converter stage is not loaded down. The second stage is a directly coupled emitter follower, which serves to

buffer the preamplifier from the signal processing circuits, described in the next section.

5. Power Supply

Power requirements for the receiver section were primarily determined by the bias requirement of the PIN photodiode, which needs 20 volts to 50 volts of reverse bias for proper operation. The signal-processing section required a dual ± 15 volt supply. In order to use a single power source, 30 volts was selected for bias voltage, and the entire receiver operates from the dual ± 15 volt supply. Decoupling of stages was accomplished with the 1Kohm resistors, and 10 uf capacitors.

C. SIGNAL PROCESSING SECTION

1. General

The function of the signal processing section is to extract only that portion of the receiver preamplifier output signal caused by reflection of the laser output from an obstruction in the detection zone. Primary design considerations for the signal processor were:

1. Response to weak signals, where signal-to-noise ratios could be expected to be as low as 3 dB.

2. A high degree of interference rejection, where interference sources could be expected to be fluorescent and incandescent light.

3. Reject signals reflected from non-obstructive targets, e. g., dust and smoke.

4. Rejection of signals caused by reflections from the target from transmitters other than the one synchronized to the receiver.

5. Employ a threshold detector that would provide a positive alarm-no alarm output.

In order to meet these objectives, it was decided to use bandpass active filters, that would satisfy requirements (1), (2), and (4), and to use a phase-locked-loop tone decoder to satisfy requirements (2), (3), and (5).

A block diagram of the signal processor section is shown in Figure 10.

2. Active Filter

Since the frequency spacing of the PRF of each transmitter-receiver pair could be separated by several hundred hertz, the primary restraint on the filters was to provide narrow enough bandwidth to reject interference caused by incandescent and fluorescent lights. Incandescent lights provide little or no interference, as their luminous output is very nearly constant, with only a slight amount of 120 Hz modulation. On the other hand, fluorescent lights create a considerable amount of interference signals in the frequency range of the transmitter-receiver pairs. The detector response signal to the fluorescent lights has a fundamental 120 Hz component, but, because

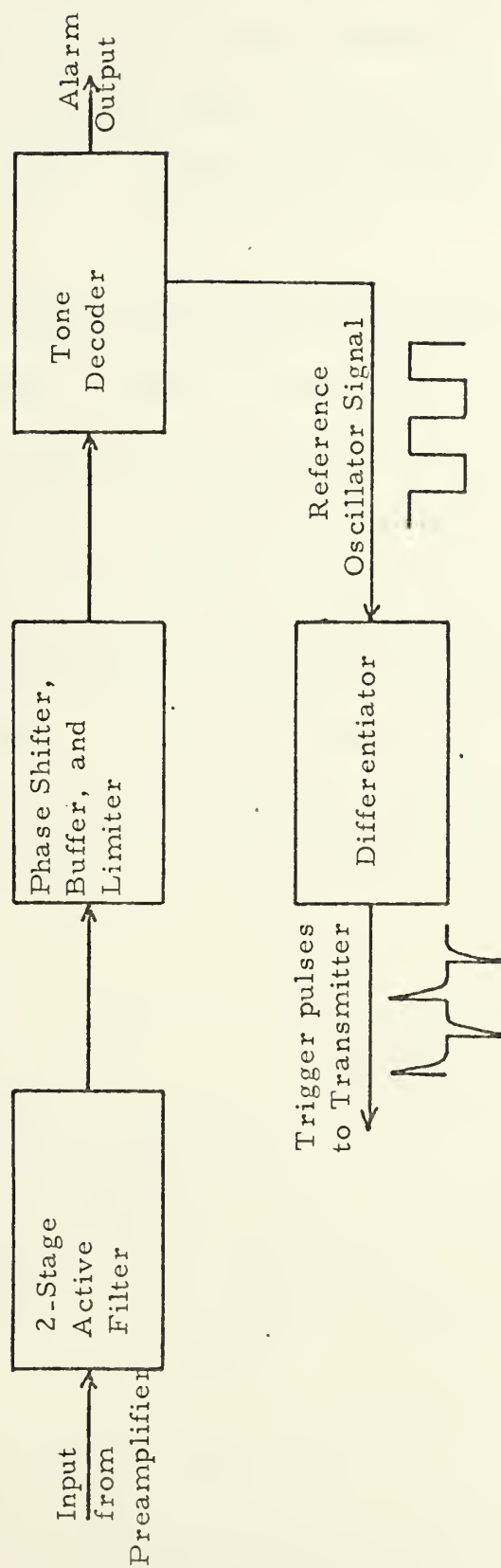


Figure 10. Signal Processor Block Diagram

of the non-linear characteristics of the gas-discharge tube, and the noise produced by the gas-discharge, the detected luminous output has frequency components extending well past 2000 Hz, and spaced every 60 Hz. Figure 11 shows a portion of the spectral content of 96" fluorescent lights.

It was therefore necessary to select operating frequencies centered between the spectral lines of the fluorescent lights. For example, an operating frequency of 1050 Hz lies between the 1020 Hz and 1080 Hz interference frequencies. Rejection of these interference frequencies was only on the order of 2 dB, but the tone decoder described in the next section provided sufficient rejection of the interference frequencies. The filters did extract the fundamental frequency of the input pulses, and provided a gain of 43.5 dB at 1050 Hz. (See Appendix B). The filters are shown schematically in Figure 12.

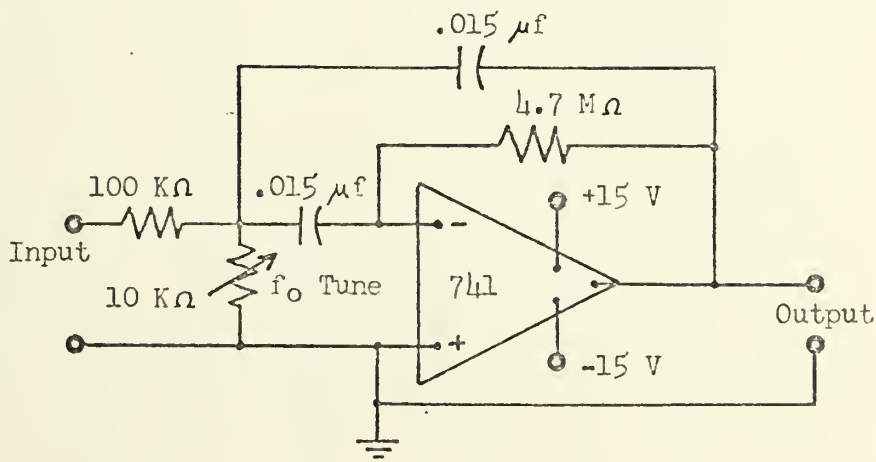


Figure 12

Active Filter Schematic
(Single Stage)

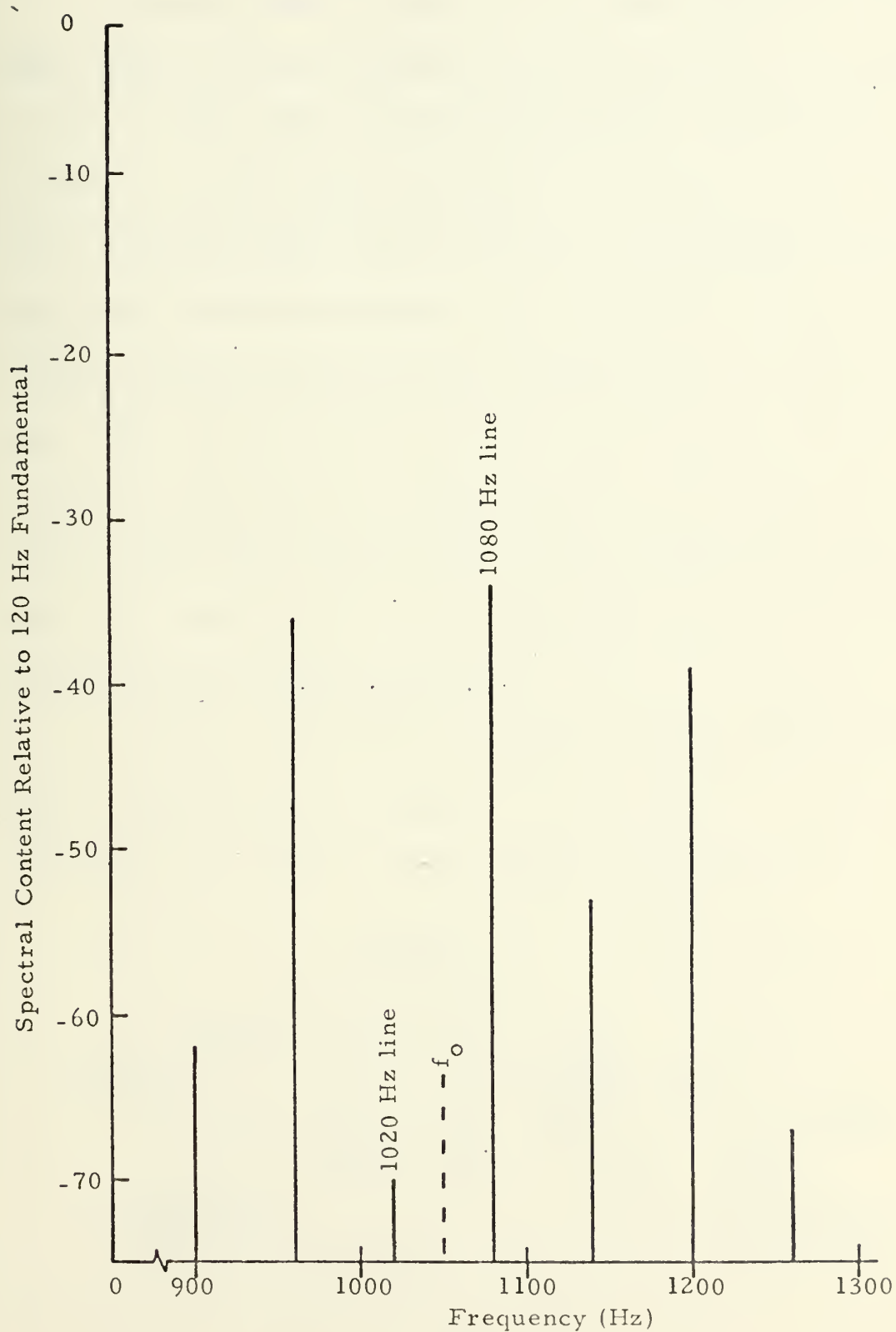


Figure 11. Portion of Spectral Content of Detected Waveform of 96" Fluorescent Lights

3. Phase-Shifter, Buffer, and Limiter

The tone decoder requires that the input signal be 90° out of phase with the reference oscillator contained within the tone decoder in order to achieve lock. In an open loop system, the reference oscillator can shift frequency (and phase) to lock onto an input signal that is within the capture range. However, in this system, since the input signal is derived from the reference oscillator, and since all circuitry preceding the tone decoder provides either 0° or 180° phase shift, the reference oscillator would shift in frequency to a point where the active filters provided a 90° phase shift, and then achieve lock. Since the filter phase characteristics were such that this frequency was on one side or the other of the amplitude response curve, a loss in overall system sensitivity resulted.

In order to eliminate this problem, an operational amplifier phase shifting circuit was employed, which provided the required 90° phase shift. The circuit is shown schematically in Figure 13.

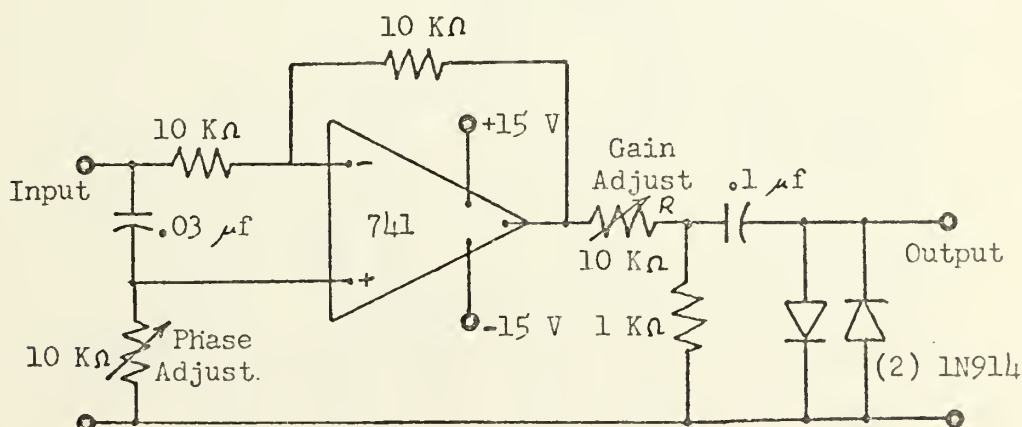


Figure 13

Phase-Shifter, Buffer, and Limiter Schematic

In addition to providing phase shift, this stage served to buffer the output of the active filter from the tone decoder, which has a low input impedance.

To prevent excessive input signal amplitude to the tone decoder, the two diodes were employed to provide hard limiting of the input signal. Signals in excess of 1.2 volts peak amplitude are clipped.

The gain control, R, provides a means of controlling the sensitivity of the receiver.

4. Tone Decoder

The final stage in the detection process employs a Signetics 567 tone decoder. This device was chosen because of the narrow capture bandwidth available, response to low amplitude input signals, and simplicity of external circuit design. The 567 also provided a convenient source for the transmitter trigger pulses. The tone decoder stage is shown schematically in Figure 14.

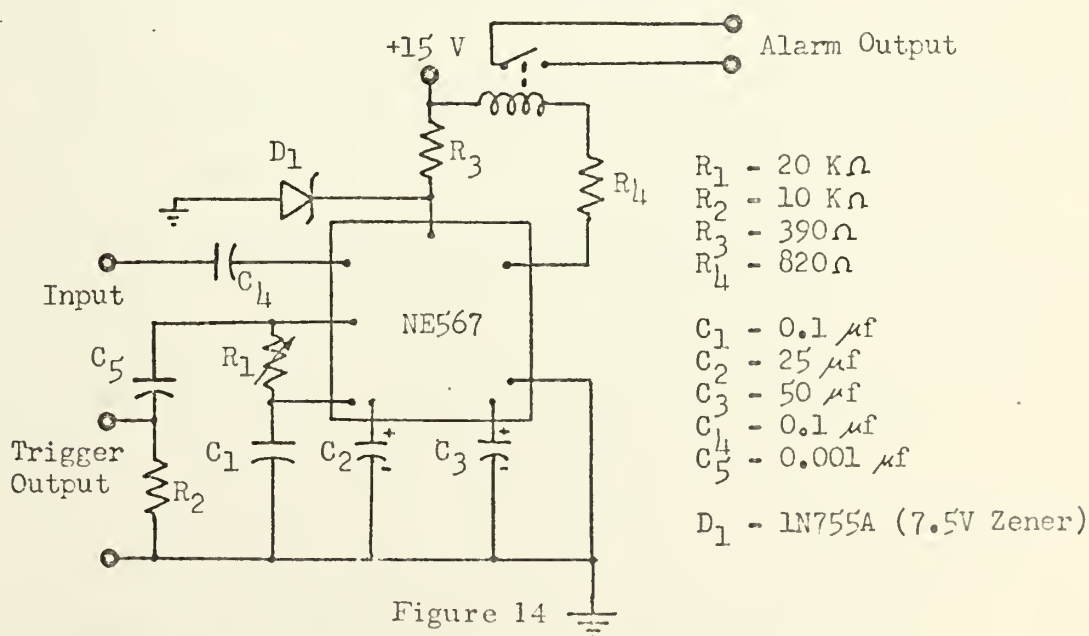


Figure 14
Tone Decoder Schematic

The circuit elements R_1 and C_1 determine the free-running frequency of the reference oscillator: R_1 is a 10 turn trimpot and was adjusted for a free-running frequency of 1050 Hz. Capacitors C_2 and C_3 control lock-on time delay, and capture bandwidth. They also interact to control the centering of the capture bandwidth (skew) about the free-running frequency. With the values specified, the capture bandwidth is skewed toward the lower frequencies; this was done in order to provide greater rejection to the 1080 Hz component of fluorescent light interference, which was 36 dB stronger than the 1020 Hz component. (See Figure 11).

Lock-on time was set at approximately 0.1 second (i. e., the tone decoder must receive about 100 cycles at the input before lock-on occurs). This was done in order to prevent false alarm conditions resulting from non-obstructive reflectors, such as dust and smoke. Reflectors such as these provide a scintillating reflection of very short duration.

The tone decoder can sink up to 100 ma when a lock condition occurs, and this sink can drive whatever suitable alarm circuit is desired. Since this portion of the tone decoder is compatible with most logic circuitry, the several tone decoders could drive a central multi-input OR gate that set an alarm condition (i. e., stop the vehicle) wherever any receiver sensed an obstruction.

The reference oscillator is the source of trigger pulses for the transmitter. This scheme has the advantage of producing

synchronous detection, since the signal that the tone decoder will respond to is generated by the tone decoder itself. Thus, any frequency drift in the reference oscillator will not degrade system performance, as long as the drift does not exceed the passband limits of the active filters. In addition, the input signal must be 90° ($\pm 5^{\circ}$) out of phase with the reference oscillator. This fact reduces the susceptibility to undesired signals, in that both the frequency and phase of the input signal must be within very close limits to produce an alarm condition.

The reference oscillator output is a five volt peak-to-peak square wave, and it was necessary to differentiate this signal to provide negative spikes of sufficient magnitude to drive the transmitter. This was accomplished with a simple RC differentiator circuit.

III. TEST RESULTS

A. RANGE TESTS

With a transmitter receiver pair arranged in the configuration of Figure 2, operating at a PRF of 1050 Hz, a positive alarm condition was achieved with a white cardboard target of 1 ft^2 area at a maximum range of 16 feet. The edges of the detection zone were sharply defined, with an edge definition of less than one inch at the 16 foot range.

In order to more fully investigate the performance of the transmitter and receiver optics, and to develop a range equation for the overall system, more extensive tests were conducted.

1. Reflection Tests

For these tests, a target of known area was positioned at various ranges from the transmitter. Range from the transmitter and receiver was the same. The target was a 1 ft^2 white cardboard square. Return signal strength was measured at the output of the pre-amplifier. Since the photocurrent of the photodiode is directly proportional to the radiant power density incident on the photodiode, relative signal strength was computed as: $10 \log \frac{v_{\text{out}}}{v_{\text{ref}}}$. Figure 15 shows the response curve of the target described. The reference, v_{ref} , was arbitrarily chosen as the output voltage with the target at a range of two feet.

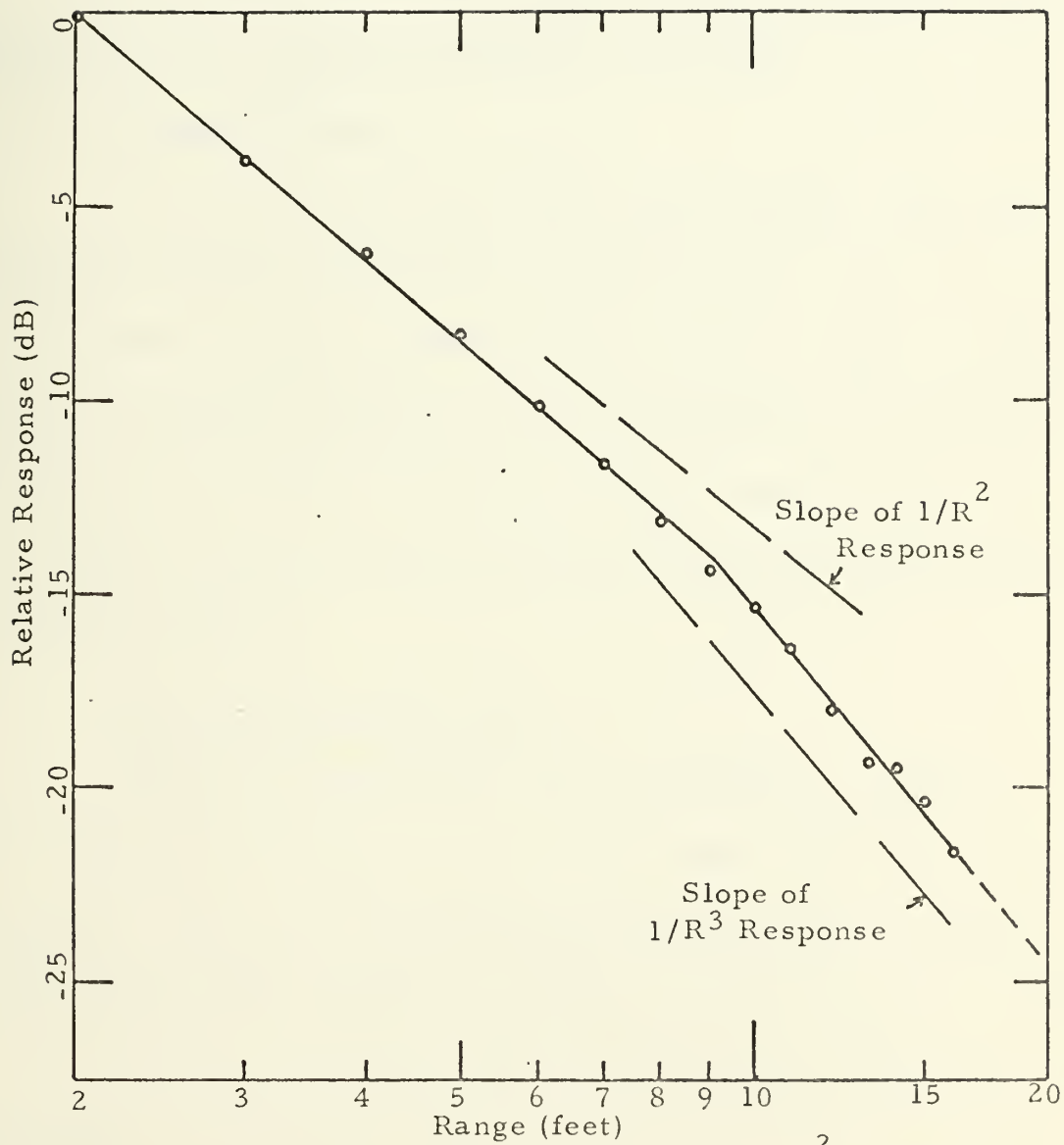


Figure 15. Range Response of a 1 ft² Target

The portion of the response curve from two feet to nine feet does not follow the $1/R^3$ response that was expected. This was caused by aperture limiting the portion of the target illuminated by the transmitter and seen by the receiver: as the range increased, effective target area also increased.

At ranges greater than nine feet, aperture limiting ceases, and the response follows the expected $1/R^3$ form.

2. Target Response

Tests of response to various target materials were made. Results are tabulated in Table II. The "half power angle" is the angle of the target (from the normal to the transmitter) at which the reflected power is reduced by one-half. For an isotropically reflecting surface, Lambert's Law would indicate that this angle should be 60° . Since this angle is less in all cases, none of the targets tested are purely isotropic reflectors.

3. Direct Line-of-Sight Tests

These tests were conducted in four phases: no optics, transmitter optics alone, receiver optics alone, and with all optics employed. They were expected to show the performance of each section of the optics employed, as well as to demonstrate the potential of the transmitter and receiver for uses other than obstruction detection.

The transmitter and receiver were aligned in a straight path line-of-sight, and again, preamplifier output was taken as a

| Target Material | Reflection Loss (dB) | Half Power Angle ($^{\circ}$) |
|-------------------------|-------------------------|------------------------------------|
| Mirror | 0 | 0 |
| Plexiglas | -2.36 | 1 |
| Aluminum Sheet | -6.8 | 3.5 |
| Plywood | -29.3 | 42.5 |
| Brown Paper | -29.8 | 45 |
| White Cardboard | -30.3 | 40 |
| Light Colored Cotton | -30.3 | 45 |
| Medium Colored Wool | -30.3 | 50 |
| Green Cardboard | -30.9 | 40 |
| Dark Colored Cotton | -31.5 | 45 |

Table II.

Relative Reflection Characteristics
of Various Targets

measure of response. The results are shown in Figure 16, and demonstrate the gain realized from the optics.

At a range of 100 feet, the transmitter optics provide a gain of 15 dB, the receiver optics provide a gain of 8 dB, and all optics combine to achieve a gain 22.5 dB.

Without optics, the range response is slightly better than the $1/R^4$ form expected. This can be attributed to the fact that the laser output is somewhat collimated as it exits the junction, and cannot be considered an isotropic source.

Figure 16 also shows the effect of saturation of the pre-amplifier stage with signals greater than about six volts (-5 dB), and the fact that the photodiode saturates at light levels greater than that required for a 20 volt (0 dB) output.

In section I. B. 1., the maximum theoretical gain of the receiver optics was calculated as 35.5 dB. Test results show a gain of 8 dB for the receiver optics. The 27.5 dB loss is attributed to the integrating surface. This loss is composed of two factors: attenuation and reflection losses of the mylar surface, and re-radiation effects from the surface. Attenuation and reflection losses could be measured directly, and were shown to amount to -4.2 dB. The re-radiation effect makes up the remaining loss. If each element of the integrating surface can be considered a point source, the solid angle from that point to the photodiode surface subtends a solid angle of only 1.39×10^{-3} steradians. Thus the theoretical loss from each point is

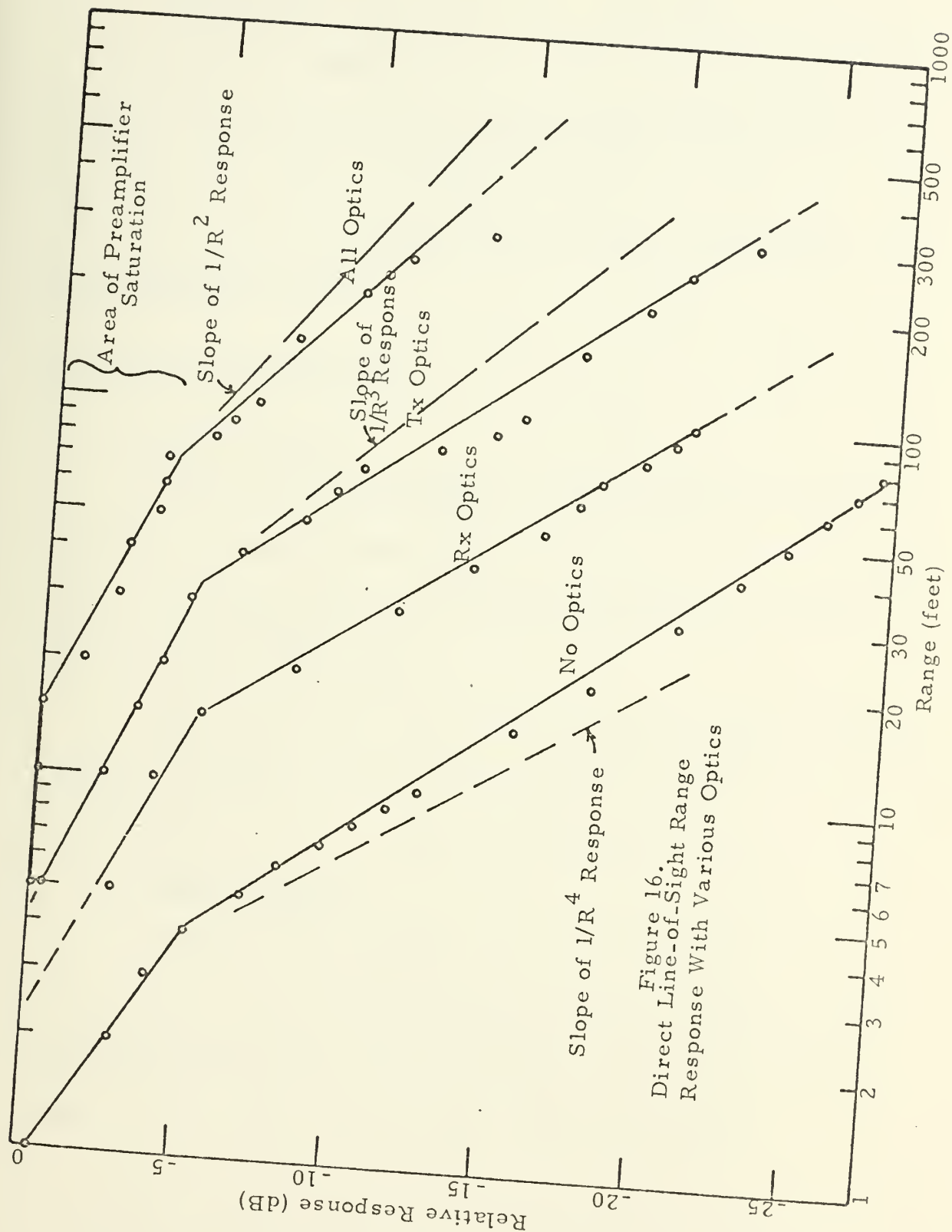


Figure 16.
Direct Line-of-Sight Range
Response With Various Optics

$$\frac{1.39 \times 10^{-3}}{2} = 2.2 \times 10^{-4} \Rightarrow -43.4 \text{ dB.}$$

The actual re-radiation loss is 23.3 dB, and the difference can be explained as arising from the fact that the target image on the surface is of finite size, which the photodiode integrates, and that some reflections from inside the aluminum mount for the integrating surface land on the photodiode surface.

B. SPURIOUS RESPONSES

1. Ambient Light

With the system operating in a high level fluorescent light environment, no false alarm conditions were encountered, as long as the operating frequencies were set between the harmonic frequencies of the fluorescent light signal.

By using a high-intensity strobe lamp, false alarm and jamming (non-response to target) could be obtained, but this type of source could not be expected to be encountered in normal service.

2. Dust and Smoke

No false alarm conditions were encountered when dense tobacco smoke was blown into the detection zone. A type of "chaff", small paper discs from a three-hole punch, was sprinkled into the detection zone, with no false alarm condition resulting.

3. Electromagnetic Compatability

The pulsing circuit emits electro-magnetic radiation fields that could be detected with a portable AM radio at distances of up to 10 feet. A plot of this radiation, measured with an AN/PRM-1 field intensity meter is shown in Figure 17.

Attempts were made to make the receiver respond to radio frequency signals. A signal generator with a 0.5 watt output was coupled to the receiver with a three inch loop of wire located six inches from the photodiode. No response was noted with the signal generator operating from 10 MHz to 250 MHz. These tests were conducted with both CW output, and with the output modulated at the operating frequency of the tone decoder.

4. Adjacent Transmitter Interference

A target was illuminated by two other transmitters, operating at 1110 Hz and 1170 Hz. These represent the closest frequency spacing that could be expected to be employed (again, centering the operating frequencies between fluorescent light harmonics). No response to either transmitter by the tone decoder was noted.



Figure 17. Radiated Interference Frequency Spectrum

IV. CONCLUSIONS

A. RANGE RESPONSE

It was assumed during the initial design phase that an $1/R^3$ response could be expected since the transmitter beam was collimated in one dimension. Test results showed that the range response followed a $1/R^3$ slope very closely.

The maximum range required was 12 feet, although minimum target size was not specified. To determine the minimum target size detectable at any arbitrary range, a range equation of the following form can be used:

$$R^3 = K\sigma$$

Where

K = a constant based on transmitter power, gain of transmitter and receiver optics, and minimum signal-to-noise ratio for valid alarm.

σ = target effective area, which depends on reflection coefficient and angle of incidence and reflection.

Using a 1 ft² white cardboard square as a target of $\sigma = 1$, the minimum effective target area is 0.422 ft² for response at a range of 12 feet.

B. TARGETS

The effective target area is a very difficult factor to predict: much like the effective radar cross-section, it is statistical in nature. Targets with a high reflection coefficient (e. g., mirrors, smooth metal, plexiglas) make poor targets since the angle of incidence and reflection is very critical. Targets of much lower reflection coefficient make better targets, since the angle can vary considerably with much less loss in effective area.

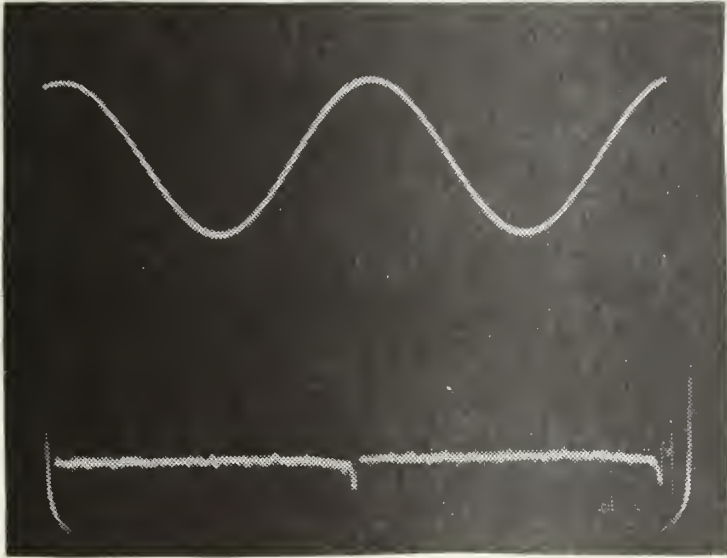
C. ENVIRONMENTAL CONDITIONS

It was intended to design a system that could operate in high ambient light conditions. This goal was achieved, largely due to the very narrow capture bandwidth of the phase-locked-loop tone decoder, which is the heart of the synchronous detection system employed.

The use of integrated circuits for the active filters and tone decoder allow the use of these types of circuits in a system of small size with modest power requirements.

APPENDIX A.

Photographs of Various Voltage and Current Waveforms



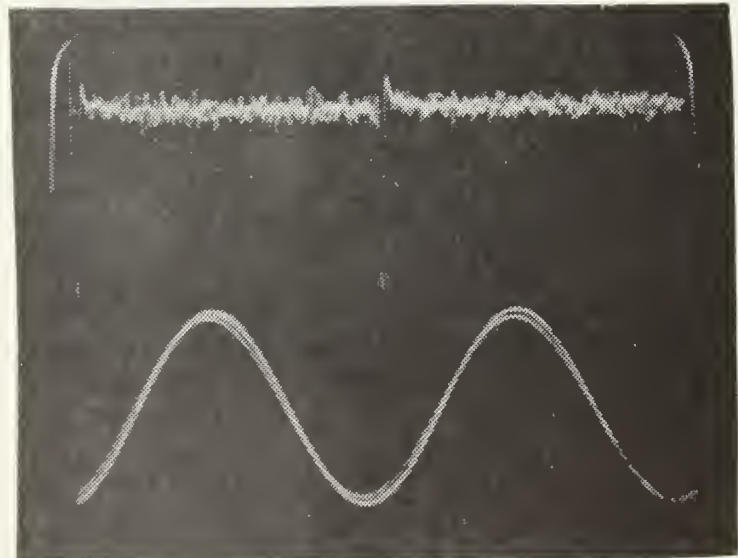
Preamplifier and
Filter Output,
High S/N Ratio.

Horiz: .2 ms/Div.

Vert:

Upper: .2 V/Div.

Lower: 1 V/Div.



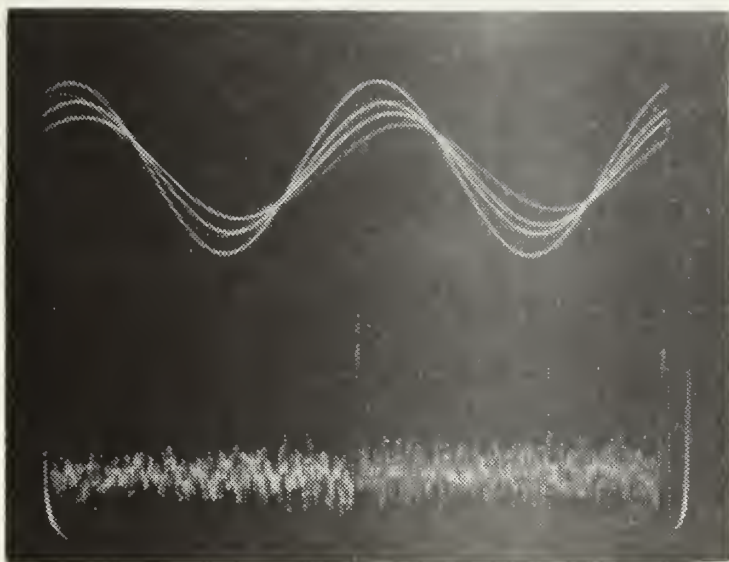
Preamplifier and
Filter Output,
Medium S/N Ratio.

Horiz: 2 ms/Div.

Vert:

Upper: .05 V/Div.

Lower: .2 V/Div.



Preamplifier and
Filter Output,
Low S/N Ratio.

Horiz: .2 ms/Div.

Vert:

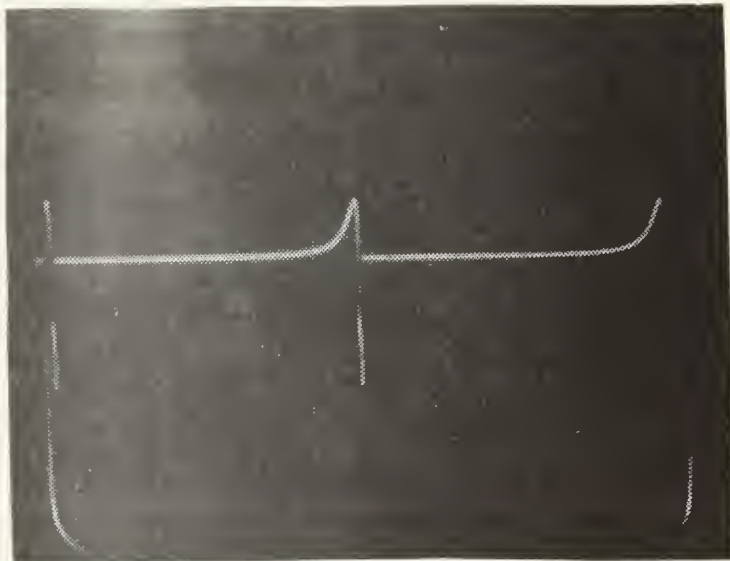
Upper: .02 V/Div.

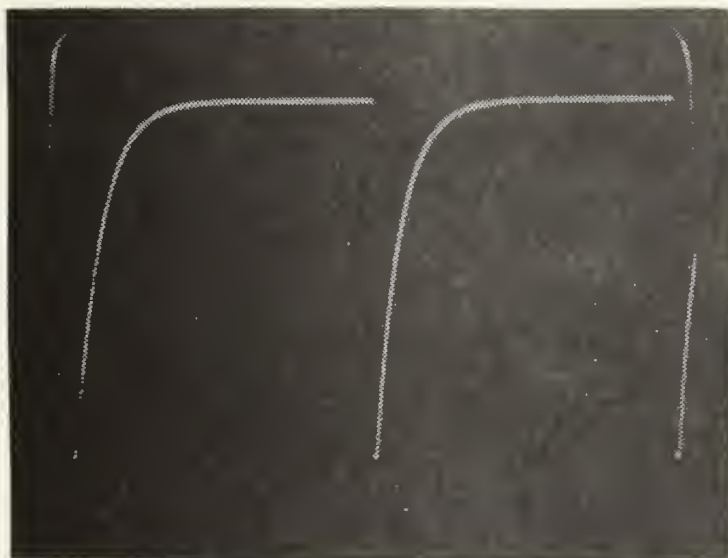
Lower: .1 V/Div.

cSCR Gate Voltage

Horiz: .2 ms/Div.

Vert: 2 V/Div.

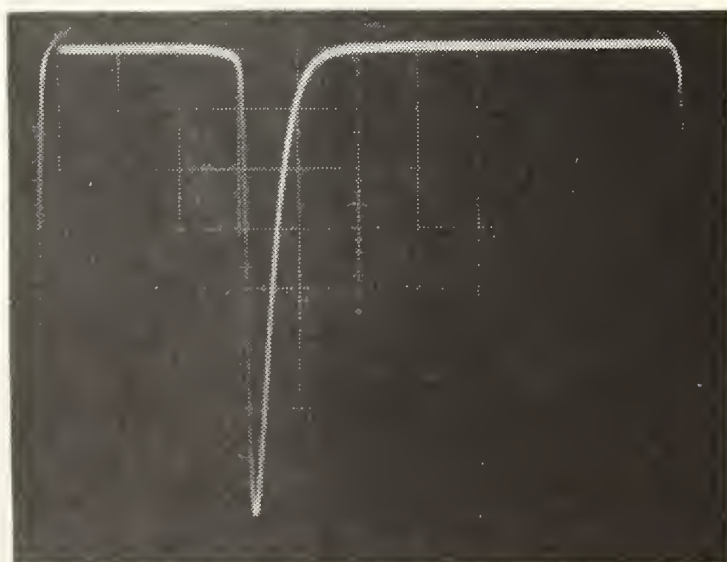




Capacitor Voltage,
 v_{cp}

Horiz: .2 ms/Div.

Vert: 50 V/Div.



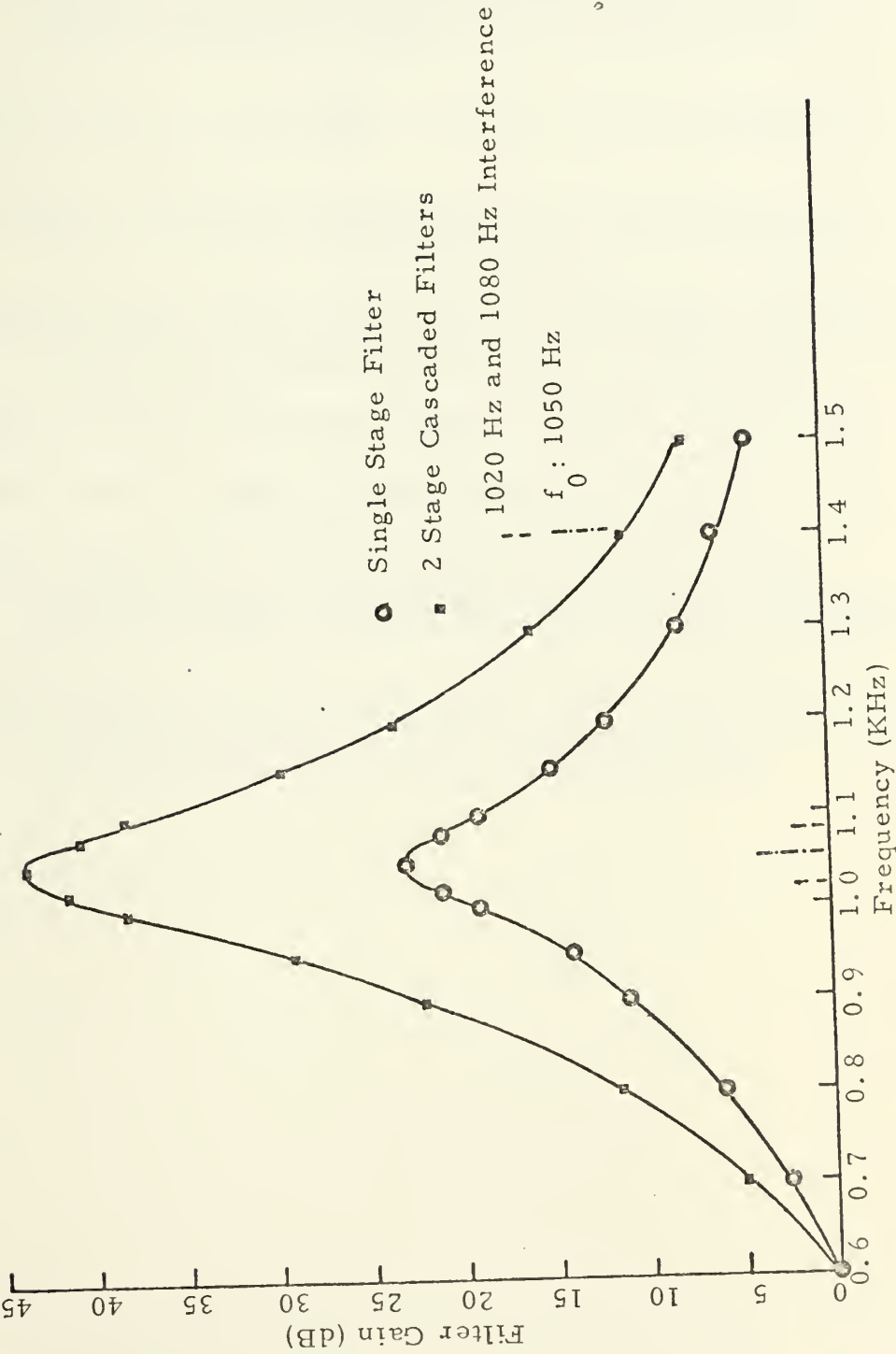
Pulsing Current, i_p .

Horiz: .5 μ s/Div.

Vert: 10 V/Div.

Appendix B

Active Filter Frequency Response



BIBLIOGRAPHY

1. Department of the Navy Publication NAVMED P-5052-35,
Control of Hazards to Health from Laser Radiation,
p. 3-4, 24 February 1969.
2. Eleccion, M., "The Family of Lasers: A Survey" Spectrum,
p. 37-39, March 1972.
3. Grebene, A. B., "The Monolithic Phase-Locked Loop - A
Versatile Building Block", Spectrum, p. 38-49, March 1971.
4. Hewlett Packard Application Note 915, Threshold Detection of
Visible and Infrared Radiation With PIN Photodiodes.
5. Hewlett Packard Application Note 917, HP PIN Photodiode.
6. Hudson, R. D., Infrared System Engineering, Wiley, 1969.
7. Radio Corporation of America Application Note AN-4469,
Solid-State Pulse Power Supplies for RCA GaAs Injection
Lasers, DeVilbiss, W. F. and Klunk, S. L., February, 1971.
8. Radio Corporation of America Application Note AN-4741,
A High Speed Pulser for Injection-Laser Diodes, De Vilbiss,
W. F. and Klunk, S. L., p. 5, September, 1971.

INITIAL DISTRIBUTION LIST

| | No. Copies |
|--|------------|
| 1. Defense Documentation Center Cameron Station Alexandria, Virginia 22314 | 2 |
| 2. Library, Code 0212 Naval Postgraduate School Monterey, California 93940 | 2 |
| 3. Assoc Professor G. L. Sackman, Code 52Sa Department of Electrical Engineering Naval Postgraduate School Monterey, California 93940 | 12 |
| 4. LT George Alfred Burman, USN Naval Electronics Systems Command (PMS116) Washington, D.C. 20360 | 1 |
| 5. Mr. Lane Lee Hewlett Packard Corporation 620 Page Mill Road Palo Alto, California 94304 | 1 |
| 6. Mr. Jack Mattis Signetics Corporation 811 E. Arques Avenue Sunnyvale, California 94086 | 1 |

Unclassified

Security Classification

DOCUMENT CONTROL DATA - R & D

(Security classification of title, body of abstract and indexing annotation must be entered when the overall report is classified)

1. ORIGINATING ACTIVITY (Corporate author)

Naval Postgraduate School
Monterey, California 93940

2a. REPORT SECURITY CLASSIFICATION

Unclassified

2b. GROUP

3. REPORT TITLE

An Optical Object Detection System for Sensing Obstructions to Low
Speed Vehicles

4. DESCRIPTIVE NOTES (Type of report and, inclusive dates)

Master's Thesis; June 1972

5. AUTHOR(S) (First name, middle initial, last name)

George A. Burman

6. REPORT DATE

June 1972

7a. TOTAL NO. OF PAGES

53

7b. NO. OF REFS

8

8a. CONTRACT OR GRANT NO.

b. PROJECT NO.

c.

d.

9a. ORIGINATOR'S REPORT NUMBER(S)

9b. OTHER REPORT NO(S) (Any other numbers that may be assigned
this report)

10. DISTRIBUTION STATEMENT

Approved for public release; distribution unlimited.

11. SUPPLEMENTARY NOTES

12. SPONSORING MILITARY ACTIVITY

Naval Postgraduate School
Monterey, California 93940

13. ABSTRACT

An object detection system to sense obstructions in the path of low speed vehicles is described. The system uses a pulsed GaAs diode laser as an illuminator, and a PIN photodiode as a detector. Reliable detection of objects with an effective area as small as 0.5 ft^2 was achieved. A signal processor using active filters and a phase-locked loop tone decoder was employed for both phase and frequency rejection of undesired signals, and detection of objects under high ambient light conditions.

14

KEY WORDS

LINK A

LINK B

LINK C

ROLE

WT

ROLE

WT

ROLE

WT

Photodiode Detector

Optical Obstruction Detection

Active Filter

Phase-Locked Loop

GaAs Diode Laser

Laser Safety Requirements

PIN Photodiode

Thesis
B88368 Burman
c.1

135765

An optical object de-
tection system for sens-
ing obstructions to low
speed vehicles.

Thesis
B88368 Burman
c.1

135765

An optical object de-
tection system for sens-
ing obstructions to low
speed vehicles.

thesB88368

An optical object detection system for s



3 2768 001 02091 0
DUDLEY KNOX LIBRARY